Gamma Ray Line Observational Results from OSSE

J.D. Kurfess, R.J. Murphy
E.O. Hulburt Center for Space Research, Naval Research Laboratory
Washington, DC 20375

M. D. Leising
Dept. Physics and Astronomy, Clemson University, Clemson, SC 29634

and W.R. Purcell
Dept. Physics and Astronomy, Northwestern University, Evanston, IL 60201

ABSTRACT. A major objective of the Oriented Scintillation Spectrometer Experiment (OSSE) on NASA's *COMPTON* Observatory is the observation of gamma ray line emission from a variety of astronomical objects. Gamma ray lines are of particular interest because they provide unique information on the production, relative abundances, acceleration and interactions of the nuclear component of matter. In this paper, we present some of the initial results obtained by OSSE on observations of line gamma-ray emission from solar flares, the galactic center region, and from supernovae.

1. Introduction

Observations of gamma-ray lines from astronomical sources has long held the promise for understanding the physical processes occurring in the most exotic and energetic objects in the universe. These include explosive objects such as supernovae and novae, compact objects such as neutron stars and black holes, the interactions of cosmic rays with matter in the interstellar medium, and the physics of solar flares. Because the fluxes of these radiations are quite low, progress has been rather slow. Nevertheless, over the past twenty years, line emission from solar flares has been observed and studied extensively with the SMM mission, positron annihilation radiation has been observed from the general region of the galactic center, and ^{56}Co emission was observed from SN 1987a.

A major objective of the Oriented Scintillation Spectrometer Experiment (OSSE) on NASA's *COMPTON* Observatory is to extend observations of gamma-ray line radiation from a variety of astronomical objects with much improved sensitivity. This is accomplished with four identical actively-shielded NaI(Tl) scintillation detectors designed to be sensitive over the 0.05 - 10 MeV energy range. Each detector has a 3.7° x 11.4° rectangular field of view defined by a passive tungsten collimator, and each has a single axis pointing control which is used to provide an offset pointing capability for background estimation. For most observations, the detectors are pointed at a source of interest for a short time (typically two minutes) and then offset to a background position on either side of the source. Summation of these 2-min background-subtracted spectra over the typical source observation of 2-3 weeks results in the best OSSE spectrum of the source. A detailed description of the OSSE instrument is given in Johnson et al. (1993)

Report Documentation Page

Form Approved
OMB No. 0704-0188

Public reporting burden for the collection of information is estimated to average 1 hour per response, including the time for reviewing instructions, searching existing data sources, gathering and maintaining the data needed, and completing and reviewing the collection of information. Send comments regarding this burden estimate or any other aspect of this collection of information, including suggestions for reducing this burden, to Washington Headquarters Services, Directorate for Information Operations and Reports, 1215 Jefferson Davis Highway, Suite 1204, Arlington VA 22202-4302. Respondents should be aware that notwithstanding any other provision of law, no person shall be subject to a penalty for failing to comply with a collection of information if it does not display a currently valid OMB control number.

1. REPORT DATE **1995**	2. REPORT TYPE	3. DATES COVERED **00-00-1995 to 00-00-1995**
4. TITLE AND SUBTITLE **Gamma Ray Line Observational Results from OSSE**		5a. CONTRACT NUMBER
		5b. GRANT NUMBER
		5c. PROGRAM ELEMENT NUMBER
6. AUTHOR(S)		5d. PROJECT NUMBER
		5e. TASK NUMBER
		5f. WORK UNIT NUMBER
7. PERFORMING ORGANIZATION NAME(S) AND ADDRESS(ES) **Naval Research Laboratory,E.O. Hulburt Center for Space Research,4555 Overlook Avenue, SW,Washington,DC,20375**		8. PERFORMING ORGANIZATION REPORT NUMBER
9. SPONSORING/MONITORING AGENCY NAME(S) AND ADDRESS(ES)		10. SPONSOR/MONITOR'S ACRONYM(S)
		11. SPONSOR/MONITOR'S REPORT NUMBER(S)
12. DISTRIBUTION/AVAILABILITY STATEMENT **Approved for public release; distribution unlimited**		
13. SUPPLEMENTARY NOTES		
14. ABSTRACT		
15. SUBJECT TERMS		

16. SECURITY CLASSIFICATION OF:			17. LIMITATION OF ABSTRACT	18. NUMBER OF PAGES	19a. NAME OF RESPONSIBLE PERSON
a. REPORT **unclassified**	b. ABSTRACT **unclassified**	c. THIS PAGE **unclassified**		**14**	

Standard Form 298 (Rev. 8-98)
Prescribed by ANSI Std Z39-18

2. Solar Flares

Solar flares are explosions that occur in the solar atmosphere leading to the emission of electromagnetic radiation (radio, visible, UV, X-rays and gamma rays), to the escape of energetic particles (electrons, neutrons, protons and heavier nuclei) and to mass ejections and shock waves. At Earth, these phenomena can cause radio blackouts, failures in the primary electrical power grid, changes in the terrestrial magnetic field and can even endanger astronauts. Because of the nearness of the Sun, the wide range of radiations produced are relatively easily detected. Solar flares therefore provide the opportunity to study in considerable detail high-energy phenomena that occur not only on the Sun, but also at many astrophysical sites where detection of the accompanying radiation is more difficult. OSSE incorporates a variety of capabilities for the detection and measurement of high-energy emission from solar flares. While solar-flare observations are not the primary mission of CGRO, excellent observations of a number of solar flares have been accomplished. In this section an overview of high-energy flare emission is given and results derived from OSSE observations of two of the flares from the remarkable June 1991 activity period are presented. The spectrum and total number of the accelerated interacting protons are derived using data from the 4 June flare and evidence is presented to support the claim that accelerated protons are stored in magnetic loops using data from the 11 June flare.

2.1. Solar Flare Gamma-ray Production

Nuclear reactions due to interactions of flare-accelerated protons and nuclei with the ambient solar atmosphere produce neutrons, gamma-ray lines and continuum emission. The principal mechanisms for the production of gamma-ray lines are nuclear deexcitation, neutron capture, and positron annihilation. The nuclear deexcitation spectrum consists of narrow lines (~2% FWHM), resulting from protons and α-particles interacting with the ambient gas, and broad lines (~20% FWHM), resulting from the interaction of accelerated carbon and heavier nuclei with ambient hydrogen and helium. Capture of the neutrons on ambient hydrogen in the photosphere produces a strong line at 2.223 MeV, and neutrons escaping from the Sun can be detected at Earth or in interplanetary space. Nuclear reactions also produce radioactive nuclei and charged pions, both of whose decay can result in positron emission. The positrons annihilate to produce a line at 0.511 MeV and a 3-photon positronium continuum. The narrow nuclear deexcitation lines and the 2.223 and 0.511 MeV lines are superposed on a continuum composed of the broad nuclear deexcitation lines and bremsstrahlung from primary electrons. Broad-band gamma-ray emission extending to high energies (>30 MeV) results from relativistic electron bremsstrahlung and from the decay of pions. Neutral pions decay directly into gamma rays, while charged pions decay via muons into secondary positrons and electrons which produce gamma rays by annihilation in flight and bremsstrahlung.

2.1.1. *Nuclear Deexcitation Lines.* The most important nuclear deexcitation lines in solar flares are listed in Table 1 along with their emission mechanisms and their principal production processes. The lifetimes of the excited states are very short ($<10^{-11}$ s) and so

TABLE 1
Solar Flare Nuclear Deexcitation Lines

Photon Energy (MeV)	Emission Mechanism	Production Processes
0.429	$^{7}Be^{*0.429} \rightarrow$ g.s.	$^{4}He(\alpha,n)^{7}Be^{*}$
0.478	$^{7}Li^{*0.478} \rightarrow$ g.s.	$^{4}He(\alpha,p)^{7}Li^{*}$
0.847	$^{56}Fe^{*0.847} \rightarrow$ g.s.	$^{56}Fe(p,p\gamma)^{56}Fe^{*}$
1.238	$^{56}Fe^{*2.085} \rightarrow {}^{56}Fe^{*0.847}$	$^{56}Fe(p,p\gamma)^{56}Fe^{*}$
1.369	$^{24}Mg^{*1.369} \rightarrow$ g.s.	$^{24}Mg(p,p\gamma)^{24}Mg^{*}$
1.634	$^{20}Ne^{*1.634} \rightarrow$ g.s.	$^{20}Ne(p,p\gamma)^{20}Ne^{*}$
1.779	$^{28}Si^{*1.779} \rightarrow$ g.s.	$^{28}Si(p,p\gamma)^{28}Si^{*}$
4.438	$^{12}C^{*4.439} \rightarrow$ g.s.	$^{12}C(p,p\gamma)^{12}C^{*}$
6.129	$^{16}O^{*6.131} \rightarrow$ g.s.	$^{16}O(p,p\gamma)^{16}O^{*}$

the time profile of such gamma-ray lines directly reflects the time profile of the proton interactions themselves. The excitation cross sections peak for interacting protons which have kinetic energies in the range 10–30 MeV.

2.1.2. *Neutrons*. The principal neutron-producing reactions in solar flares are proton-proton, proton-α particle and α particle-α particle. The neutrons which remain at the Sun either decay or are captured by nuclei, most importantly on ^{1}H to produce a 2.223 MeV gamma ray. Because of the time required for the neutrons to slow down and be captured, the gamma-ray line is delayed by about 100 seconds from the time of neutron production. A competing capture reaction is $^{3}He(n,p)^{3}H$ which produces no radiation but can affect the time-dependent flux of the 2.223 MeV line. Observations of this line can therefore set constraints on the photospheric $^{3}He/H$ ratio. The kinetic energies of the protons producing the neutrons responsible for the observed 2.223 MeV line are in the range 30–100 MeV. The ratio of the total 2.223 MeV line fluence to that of a deexcitation line is therefore sensitive to the hardness of the flare-averaged proton kinetic-energy spectrum in the 10 to 100 MeV range.

2.1.3. *Positrons.* Positrons are created in solar flares from the decay of radioactive nuclei and π^{+} mesons and from deexcitation of excited nuclei produced by the accelerated-particle interactions. Once created, the positrons slow down and annihilate with ambient electrons. Depending on the density and temperature of the ambient medium, positrons and electrons can annihilate either directly or after forming positronium. Positronium can form in either of two spin states–a singlet state 25% of the time which decays into two 0.511 MeV photons, or a triplet state 75% of the time which decays into three <0.511 MeV photons. The principal positron-emitting sources expected to be produced in solar flares are $^{16}O^{*}$ for very steep accelerated-particle spectra and ^{15}O and ^{11}C for more typical solar spectra. The mean lives of the positron emitters vary from 10^{-10} seconds for ^{16}O to 1760 seconds for ^{11}C. Positrons also result from the decay of π^{+} mesons produced primarily in p-p and p-α interactions. The π^{+} mesons decay into muons which, in turn, decay into positrons. The half-lives of these particles are very short (2.6 x 10^{-8} s

for the π^+ and 1.5 x 10^{-6} s for the μ^+) but the initial energies of the positrons are larger (10–100 MeV) than those of positrons from radioactive nuclei (<1 MeV) and so the slowing-down times can be longer. The threshold energy for pion production is >200 MeV and for very hard proton kinetic-energy spectra, these sources of positrons can dominate. Since the annihilation line is composed of a superposition of radiation from many sources with a variety of half-lives, the time-dependence of the 0.511 MeV line can be complex and not easily related to the proton interaction time profile.

2.1.4. *High-energy Emission.* At energies greater than ~10 MeV, most of the gamma rays in solar flares are expected to be produced by electron bremsstrahlung and π° decay with some additional contribution from bremsstrahlung of π^+- and π^--decay positrons and electrons. Neutral pions decay with a half-life of less than 10^{-15} s into two gamma rays with energies of 67.6 MeV in the pion rest frame. The energies of these photons are then Doppler shifted by the pion motion but, for the energetic-particle spectra associated with solar flares, nearly all of the Doppler-shifted radiation remains above ~30 MeV. The spectrum is a broad peak centered at ~70 MeV with a FWHM of ~100 MeV (Crannell, Crannell and Ramaty 1979). The time profile of this prompt pion-decay radiation reflects the time profile of >200 MeV proton interactions. The positrons (electrons) resulting from $\pi^+(\pi^-)$ decay have initial energies from 10 to 100 MeV and as these positrons and electrons slow down and thermalize in the solar atmosphere they produce bremsstrahlung radiation, much of which is at photon energies greater than 10 MeV.

2.2. The June 1991 Solar Flares

In June, 1991, solar active region 6659 produced several of the largest GOES flare events ever recorded by the satellites. Two of these flare are discussed here. On 4 June, AR 6659 produced an X12+ flare while OSSE was viewing the Sun. (X12+ flares are major solar events in which the 2-6 A X-ray flux exceeds the maximum detection range of the X-ray monitors on the GOES satellites. They typically occur only several times during each solar cycle). Excellent observations were obtained of the rise, peak and decay of the event. The decay was interrupted by spacecraft night, but observations were resumed at sunrise of the next two orbits and additional observations were obtained. On 11 June, AR 6659 produced another X12+ flare. At the time, OSSE was viewing in the Cygnus region but immediately slewed to the Sun in response to a BATSE solar flare trigger. Solar observations continued for over 3000 seconds until the detectors slewed back to Cygnus and were then resumed during the next orbit. In both cases, the instrument was configured to obtain a range of solar data. Here we use count-spectrum data covering the energy range from 0.05 to 10 MeV in 512 channels.

2.2.1. *The 4 June 1991 Flare*. Figure 1 shows a count spectrum from the 4 June flare accumulated after the peak of the flare emission. The sources of the prominent spectral features are indicated. Using a combination of data from on- and off-pointed detectors, we have determined the fluxes of both the 2.223 MeV neutron-capture and the 4.44 MeV ^{12}C nuclear-deexcitation lines throughout the observable emission period. The time-integrated fluences of these lines are 850±14 and 128±13 photons cm^{-2}, respectively. We

use recent theoretical calculations (Ramaty et al. 1993; Kozlovsky, Murphy and Ramaty 1994) to derive estimates for the flare-averaged kinetic-energy spectrum of the interacting, accelerated particles (using the 2.223-to-4.44 MeV line fluence ratio) and the total number of interacting protons (using the total 2.223 MeV line fluence). Since the data coverage is incomplete, the total-number estimate will be a lower limit. The ratio, however, should be reasonably independent of the unknown emission profile during the data gaps. Assuming a power-law form for the particle spectrum, we find that the measured ratio (6.6±0.7) implies an index of ~3.1, independent of either the assumed angular distribution of the interacting particles or the assumed abundances. This can be compared to indices calculated for a number of flares by Ramaty et al. (1993) using a similar technique. Their values ranged from 2.7 (for the 16 December 1988 flare) to 4.5. (Note: Their derived index for the large flare of 4 August 1972 was 3.4–3.7.)

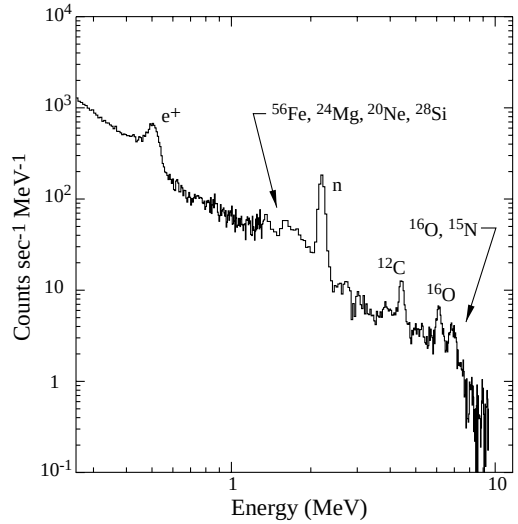

Figure 1. OSSE count spectrum from the 4 June 1991 solar flare.

The implied number of interacting protons with energy greater than 30 MeV [N_p(>30 MeV)] depends somewhat on the assumed abundances at the interaction site. Using photospheric abundances (Anders and Grevesse 1989) for both the ambient and accelerated particles, the measured 2.223 MeV line fluence implies N_p(>30 MeV) ~3×10^{33}. Using the enhanced-heavy-element abundances derived (Murphy et al. 1991) for the 27 April 1981 flare observed by *SMM*/GRS, we find N_p(>30 MeV) ~7×10^{32}. We emphasize again that these are lower limits since we have not accounted for emission during data gaps. These values can be compared to those derived for a number of flares by Ramaty et al. (1993) which ranged from 1.6×10^{30} to 1×10^{33} (for the 4 August 1972 flare). We see that the 4 June 1991 flare was comparable in size to the 4 August 1972 flare but had a harder spectrum.

2.2.2. *The 11 June 1991 Flare.* The 11 June flare is unique in that EGRET has reported observing high-energy (>50 MeV) emission many hours after the peak of the X- and gamma-ray emissions. Mandzhavidze and Ramaty (1992) have analyzed the EGRET data and found that this late emission can be fit with a combination of pion-decay radiation and primary electron bremsstrahlung. They argue for a model in which the bulk of the particles responsible for the late, high-energy emission are accelerated during the impulsive phase and are subsequently trapped in coronal magnetic loops. Since the lower-energy particles responsible for nuclear-line emission are expected to lose their energy faster than the higher-energy particles responsible for the pion-decay emission, a consequence of such a model is that the nuclear-line emission should decay faster than the high-energy emission.

If the high-energy emission is due to continuously-accelerated particles, the two types of emission should have comparable time profiles.

The most reliable measure of nuclear-line emission would be a fit to a prompt narrow nuclear line, such as the 4.44-MeV ^{12}C line. At the late times of interest in the 11 June flare, the flux in such a line is expected to be quite weak. An alternative is to fit the broad, nuclear-dominated energy range from ~1 to 9 MeV with a model of the narrow-line nuclear spectrum. Such an analysis approach is currently being completed. Here we use the 2.223-MeV neutron-capture line time profile to estimate the nuclear-emission time profile. As mentioned above, this line is delayed relative to that of the nuclear reactions themselves. However, this delay is on the order of ~100 seconds, which is much less than the time scales of interest here (hours). The neutron-capture line time profile, therefore, should provide an adequate measure of the nuclear-line production time profile. We have used OSSE data obtained after the peak of the 11 June flare to avoid data problems near the flux maximum. The data from each of the two detectors which were continuously pointed at the Sun were summed into 4 time bins: two bins after the peak but during the same orbit as that of the peak, and two bins during the following orbit. The count spectra near the region of the neutron-capture line were then fit with a narrow Gaussian line centered at 2.223 MeV.

Figure 2 (from Mandzhavidze and Ramaty, 1992) shows the EGRET data from the 11 June flare (the peak of the GOES soft X-ray emission occurred at 2:09 UT). The solid and dotted curves shown in the figure are fits by Mandzhavidze and Ramaty to the EGRET high-energy data (Kanbach et al. 1993) assuming impulsive acceleration. The dashed curve is their prediction for the 4.44-MeV nuclear line. The parameters listed in the figure relate to their loop model. We have overplotted the OSSE measurements of the 2.223-MeV line, renormalized such that the earliest OSSE measurement falls on the predicted 4.44-MeV line curve. The predicted curve is consistent with the OSSE observations providing support for the conclusion that the particles are accelerated impulsively. It must be noted, however, that high-energy particles trapped in magnetic loops and producing pions will also produce neutrons, although not as efficiently as the

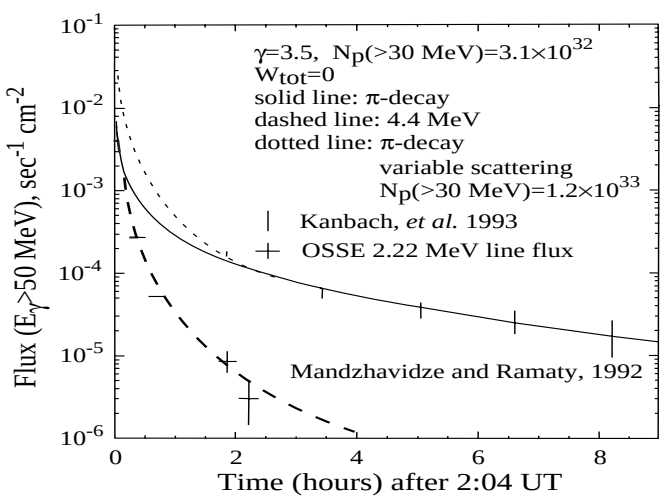

Figure 2. Measured and calculated time-dependent fluxes of the >50 MeV gamma rays and predicted 4.44 MeV gamma rays from the 11 June 1991 solar flare (from Mandzhavidze and Ramaty 1991). Also shown are the renormalized OSSE measurements for the 2.22 MeV neutron-capture line for this flare.

lower-energy particles. It would be expected, then, that even under the trapped-particle scenario the neutron-capture line time profile will be similar to that of the high-energy emission at late times in the flare. Comparison of the OSSE data with the high-energy curve shows that this is not the case for the time period covered by the OSSE data, implying that the bulk of the emission at these times is produced by particles accelerated impulsively.

3. Galactic Positron Annihilation Radiation

3.1 Positron Production and Annihilation

Positrons can be produced by several different mechanisms, including: cosmic-ray interactions in the interstellar medium (Lingenfelter & Ramaty 1982); gamma-ray bursts (Lingenfelter & Hueter 1984); pulsars (Sturrock 1971); β^+-decay products from radioactive nuclei (e.g., ^{56}Co, ^{44}Sc, and ^{26}Al) produced by supernovae, novae, or Wolf-Rayet stars (Clayton 1973; Ramaty & Lingenfelter 1979; Signore & Vedrenne 1988; Woosley & Pinto 1988; Lingenfelter & Ramaty 1989); and photon-photon pair production in the vicinity of an accreting black hole (Lingenfelter & Ramaty 1982; Rees 1982; Ozernoy 1989; Ramaty et al. 1992). Regardless of the positron production mechanism, however, the positrons will eventually interact with electrons, resulting in the annihilation of the positron-electron pairs and in the production of gamma rays. The energy of the resulting photons depends on the details of the annihilation process.

As discussed in Section 2.1.3, a positron can annihilate with an electron either directly or through the formation of positronium. Direct annihilation results in the production of two 511 keV ($=m_ec^2$) photons in the center of mass frame. Annihilation via positronium results in the emission of two 511 keV photons in the C.M. frame if the positronium was formed in the singlet quantum state. If the positronium was formed in the triplet quantum state, three photons are emitted whose total energy equals 1022 keV ($=2m_ec^2$). The shape of the resulting continuum emission is roughly triangular, increasing from zero at 0 keV to a maximum at 511 keV (see the positronium continuum component shown in Figure 3). The positronium fraction, f, provides a measure of the fraction of positrons that annihilate through the formation of positronium and is given by (Brown & Leventhal, 1987):

$$f = \frac{2.0}{[2.25*(I_{511}/I_{pos}) + 1.5]}$$

where I_{511} is the observed number of photons in the 511 keV line and I_{pos} is the observed number of photons in the positronium continuum. A value of f = 1 indicates that all of the positrons annihilate through the positronium channel while a value of f = 0 indicates that none of the positrons annihilate through the positronium channel. The properties (i.e., temperature, density, ionization fraction) of the medium in which the positrons annihilate can affect the positronium fraction (Guessoum, Ramaty & Lingenfelter, 1991). For annihilation in cold clouds, the positronium fraction is expected

to be 0.9, independent of the amount of dust in the clouds. For annihilation in the warm interstellar gas, the positronium fraction is expected to be 0.9, unless there is significant dust in which case the positronium fraction may be much lower. Annihilation in the hot interstellar gas will result in a positronium fraction < 0.5.

3.2 Previous Observations

Numerous observations of positron annihilation from the direction of the Galactic center have been performed over the past 20 years (see the recent reviews by Tueller 1993; Skibo, Ramaty & Lingenfelter 1994; Lingenfelter & Ramaty 1989). These observations have utilized various types of detectors and have included both satellite and balloon-borne instruments. Nearly all of these observations have resulted in positive detections of a 511 keV line characteristic of positron annihilation. The line centroid and width have been measured using high resolution Ge-based detectors. The line is found to be within 0.5 keV of 511 keV and to have a full-width at half-maximum (FWHM) of 2.5 +/- 0.4 keV (Leventhal et al. 1993). The intensity of the line has been found to be positively correlated with the instrument field-of-view, indicating there is a diffuse component to the observed emission (see Teegarden 1994). There have also been reports of time-variability in the 511 keV line flux when the Galactic center region was observed at different times by the same instrument, suggesting there may also be a point source component to the observed emission.

One possibility for a point source of positrons is the black hole candidate 1E 1740.7-2942. Observations by the SIGMA instrument on the GRANAT spacecraft have identified 1E 1740.7-2942 as an extremely time variable hard X-ray source (Churazov et al. 1993). On 1990 October 13-14, the SIGMA instrument observed a strong flare from 1E 1740.7-2942 which exhibited an intense ($\sim 10^{-2}$ photon $cm^{-2}s^{-1}$), broad line feature (FWHM 240 keV) with an energy of ~470 keV (Bouchet et al. 1991). This feature has been interpreted as a broadened, red-shifted 511 keV line resulting from positron annihilation occurring in an accretion disk surrounding 1E 1740.7-2942 (Sunyaev et al. 1991; Ramaty et al. 1992). Similar outbursts were observed by SIGMA in 1991 October and 1992 September (Cordier et al. 1993), though a simultaneous observation of the Galactic center region by the OSSE instrument during the 1992 September outburst did NOT detect the reported excess (Jung et al. 1994). There is no direct evidence, however, that the transient line feature observed by SIGMA is related to the narrow 511 keV line which has been observed since the early 1970's. Further, both the SIGMA and GRIP instruments have provided 95% confidence upper limits of $\sim 4 \times 10^{-4}$ photons cm^{-2} s^{-1} for time-averaged narrow 511 keV line emission from 1E 1740.7-2942 (Lei et al. 1993, Heindl et al. 1993).

3.3 OSSE Observations and Results

The OSSE instrument provides the unique ability to perform high-sensitivity observations of the Galactic plane and Galactic center region to measure the distribution of positron annihilation radiation and to search for time variability of the emission. The OSSE

observations of the Galactic plane and Galactic center region have been used to investigate the distribution of the diffuse 511 keV line emission and to search for possible time variability of the emission. A spectrum from one of the OSSE observations of the Galactic center is shown in Figure 3. This spectrum shows strong evidence for a narrow 511 keV line and positronium continuum, with an underlying continuum component. The position of the line is consistent with an energy of 511 keV and the line width is consistent with the instrumental resolution. The positronium fraction for this spectrum is 0.94 +/- 0.04.

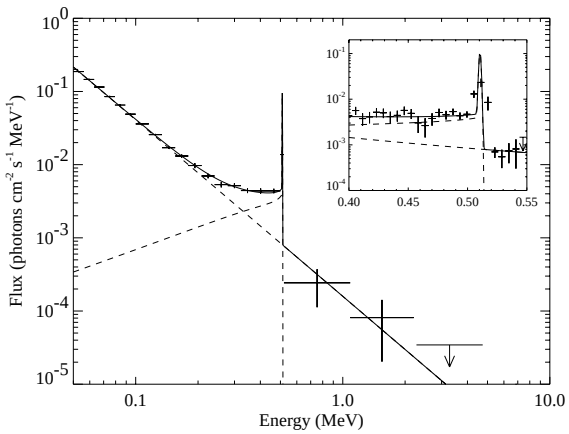

Figure 3. The OSSE galactic center spectrum from the July, 1991 observation. The fitted function consists of a power law, a photopeak line fixed in energy and width at 511 keV and 2.5 keV, respectively, and a positronium continuum component. The dashed lines indicate the contribution of each component.

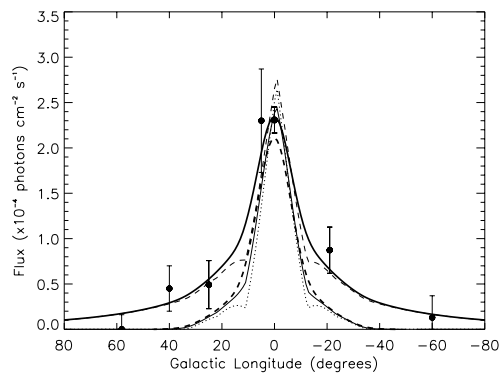

Figure 4. The Galactic longitude distribution of the 511 keV line emission as observed by OSSE. The curves represent the expected OSSE responses for several galactic distribution models, each fitted simultaneously to all of the galactic center and galactic plane data.

The Galactic longitude distribution of the narrow 511 keV line emission observed by OSSE shows that the emission is strongly peaked in the direction of the Galactic center, as shown in Figure 4. When combined with other OSSE data from observations of the Galactic center and Galactic plane, the 511 keV line distribution is found to be best described by a two-component model consisting of a Galactic disk and a nuclear bulge component. This distribution model is also consistent with most of the observations of narrow 511 keV line emission reported by other instruments, as shown in Figure 5. Using the combined data set, all other distribution models investigated can be excluded at the > 4.5 sigma level (Purcell et al 1994).

There is no evidence for significant time variability of the 511 keV line flux during the OSSE observations of the Galactic center region. A limit of ~1-2 x 10^{-4} photons cm^{-2} s^{-1} can be placed on a time-variable component of the 511 keV line emission during the OSSE observations of the Galactic center region. The best-fit distribution model can also be compared with previous results by other instruments to place historical limits on the

time variability of the 511 keV line emission; there is no evidence for significant time-variability, as shown in Figure 5. A limit of ~ 4 x 10^{-4} photons cm^{-2} s^{-1} can be placed on a historical time-variable component of the 511 keV line emission.

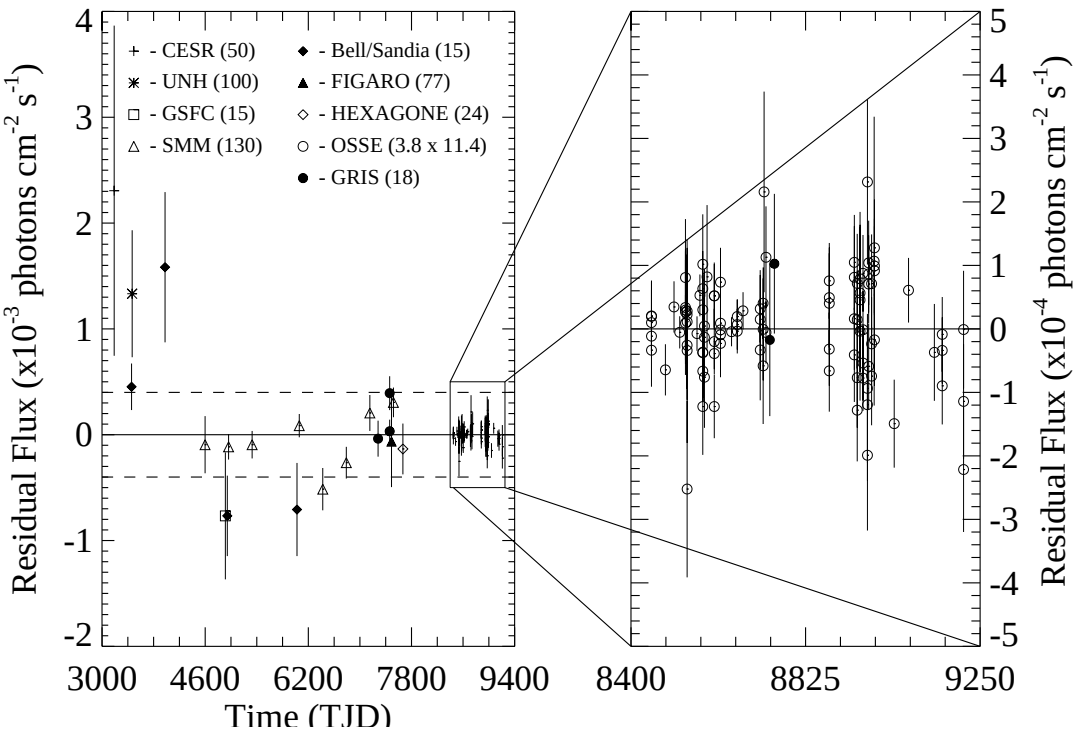

Figure 5. The history of the 511 keV line flux from the galactic center region as observed by various balloon and satellite instruments. Note that the uncertainties represent the statistical uncertainties only. The diffuse contribution for the best-fit Free Spheroidal model has been subtracted from the reported flux for each observation. The numbers in parenthesis indicate the field-of-view of each instrument, in degrees.
References: SMM (Share et al. 1990); GRIS (Gehrels et al. 1991; Leventhal et al. 1993); Bell/Sandia (Leventhal et al. 1986 and ref. therein); FIGARO (Neil et al. 1990); HEXAGONE (Chapuis et al. 1991); CESR (Albernhe et al. 1981); UNH (Gardner et al. 1982); GSFC (Paciesas et al. 1982)

There is also no evidence in the OSSE data for time-averaged narrow 511 keV line emission from the black hole candidate 1E 1740.7-2942. For the best-fit diffuse distribution model, the 95% confidence upper limit to time-averaged 511 keV line emission from 1E 1740.7-2942 is ~10^{-4} photons cm^{-2} s^{-1} during the OSSE observations of the Galactic center region (Purcell et al. 1994).

The OSSE observations have shown for the first time that the galactic 511 keV line emission is highly concentrated in the direction of the Galactic center and that there appears to be two components to the distribution, a galactic disk component and a nuclear bulge component. These two components may represent two different populations of

positron production sites. A large fraction of the disk component is probably due to the radioactive decay of ^{26}Al, which has been observed by both OSSE and COMPTEL (Diehl et al 1994; Leising et al 1994). The remaining positrons may be created by the radioactive decay of ^{56}Co and ^{44}Sc (synthesized as ^{44}Ti), which are thought to be produced primarily in Type Ia supernovae. The positronium fraction observed by OSSE also indicates that the annihilation is not predominantly occurring in the hot interstellar gas or in a warm, dusty medium. Further observations to map the distribution of the positronium fraction and to identify any variations in the positronium fraction may provide additional insights into the properties of the annihilation medium.

4. OSSE Observations of Supernovae

Supernovae have long been discussed as promising gamma-ray line targets (e.g., Clayton, Colgate, and Fishman 1969). Supernovae of Type Ia, having no hydrogen evident in their spectra and therefore little or no stellar envelopes, can be detected to the largest distances. They are thought to result from the complete thermonuclear disruption of degenerate dwarfs with masses near the Chandrasekhar mass, producing, to within a factor of 2, 0.5 $M_\bullet$ of radioactive ^{56}Ni. The decay of the daughter ^{56}Co ($\tau_{1/2}$=78 days) produces a number of potentially observable gamma-ray lines, and together with the decay power of ^{56}Ni, dominates the optical display. The gamma rays begin to escape from the rapidly expanding ejecta in significant numbers after just a month or so, and their fluxes peak at 2-3 months.

All of the other spectroscopic types of supernovae (Type II, Ib, Ic) probably result from core collapse in massive stars. The shock wave generated by the rebound heats and ejects whatever overlying stellar envelope there is. The heating produces roughly 0.1 $M_\bullet$ of ^{56}Ni in the slowest (innermost) ejected matter. Significant escape of gamma rays must await the thinning of the ejecta, which for massive stellar envelopes takes of the order of a year. Stellar mass loss reduces the ejecta mass and will cause the gamma-ray line peak to be brighter and earlier. Other interesting gamma-ray emitting radioactive isotopes are produced in smaller numbers in both types of supernovae. Longer-lived isotopes can survive until the ejecta are quite thin to gamma rays, and possibly give detectable fluxes after ^{56}Co has decayed away.

OSSE has had the opportunity to observe both types of events relatively nearby. In fact two core collapse events and one thermonuclear explosion have been OSSE targets. Supernova 1987A was the first individual object outside the solar system detected in gamma-ray lines (Matz et al. 1987), namely those of ^{56}Co decay. OSSE could not observe this event until 1600 days after the explosion, so ^{56}Co had decayed below the sensitivity threshold, but it was able to detect the 122 keV line and associated Compton continuum from the decay of ^{57}Co ($\tau_{1/2}$=270 days) (Kurfess et al. 1992). The detection confirmed details of calculations of the nuclear burning, but the amount of ^{57}Co was too small, by a factor of 3, to account for the optical luminosity at the time. The observed luminosity had indeed been attributed to ^{57}Co decay, but the OSSE observations required

another explanation. Stored ionization energy and dissipation of mechanical energy were suggested as strong possibilities (Clayton et al. 1992).

Supernova 1991T occurred in the spiral galaxy NGC 4527, thought to be at a distance of 10-15 Mpc, just about the time of the launch of the Compton Observatory. Both OSSE and COMPTEL observed this Type Ia supernova multiple times during the following 6 months in the hope of detecting the strongest ^{56}Co decay lines at 847 keV and 1238 keV. No significant flux was seen in either line, with both experiments setting upper limits near 4×10^{-5} photons cm^{-2} s^{-1} (Leising et al. 1994a; Lichti et al. 1994). The non-detection could be because the thermonuclear models are in error, but of course it could just be because the actual distance is near the larger end of the allowed range. It is not quite so simple, because the distance to SN 1991T can not be taken to be arbitrarily large. Any given model, to be considered in the running for explaining SN 1991T, has to give the observed brightness (B=10.6 mag at peak) after correcting for extinction, of which there was some. This constrains the distance for a given model and makes a prediction for its gamma-ray flux. Figure 6 shows this relationship, the 847 keV line flux versus the extinction-corrected peak B, for several models from the literature (see Leising et al. 1994a and references therein). The vertical lines enclose the range of the uncertain extinction correction. The horizontal lines show the COMPTEL (lower, dashed line) and OSSE (upper, dot-dash line) upper limits to the flux. None of the models explain the observations very comfortably, but clearly those which expand more slowly and trap more gamma rays, and are therefore optically brighter and gamma-ray fainter, are preferred. Also, smaller values of the extinction bring more models into agreement with the observations.

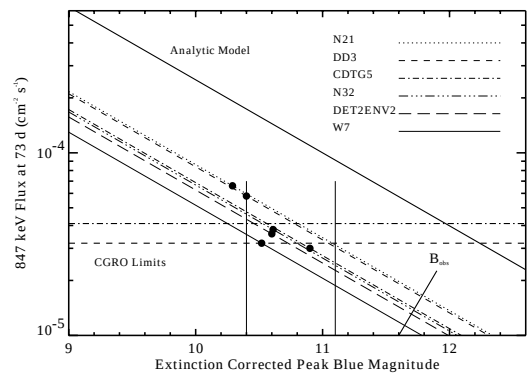

Figure 6. The peak 847 keV flux versus peak intrinsic blue magnitude for several supernova models.

Supernova 1993J occurred in the nearby galaxy M81 in late March 1993. It was peculiar from the beginning, in both its spectral evolution and its light curve. OSSE observed the supernova early (9-15 days after explosion) and often (also 23-37 days and 93-121 days). It is now, but was not then, clear that this event was a core collapse in a star which has lost almost all of its hydrogen envelope (except for ~0.1 $M_\bullet$) before it exploded. Thus at the distance of 3.6 Mpc, even 0.1 $M_\bullet$ of ^{56}Ni could not have been detected in the ^{56}Co gamma-ray lines by OSSE. The observed optical light curve suggests that slightly less ^{56}Ni was ejected. However, OSSE did detect hard X-ray photons in the first observation, and found a hint of them also in the second (Leising et al. 1994b). Fitted with a thermal bremsstrahlung model, the indicated temperature was T=10^9 K, and the 50-150 keV luminosity was 5.5×10^{40} erg s^{-1}. ROSAT and ASCA had both detected this supernova at about the same time as OSSE.

A model which could explain those observations was one in which the ejected supernova material is shocked as it is slowed when it runs into the presupernova wind. The ejecta could be heated to $T=2x10^8$ K, and its relatively high density would give a large free-free luminosity, but it would not yield a detectable photon flux in the OSSE energy range. Similarly, the circumstellar wind would be shocked by the expanding ejecta, and to an even higher temperature, but it would have low density and therefore low free-free emissivity. The OSSE observations have caused theorists to rethink the models. The OSSE spectrum seems a simple extension of the lower energy spectra, and so probably only a single emitting component is indicated. The high temperature suggests that it must be the shocked wind, but then the higher luminosity shocked ejecta must somehow be hidden, or eliminated. Continuing modelling efforts are needed to clarify this situation.

5. Summary

During the first two years of the COMPTON Observatory mission, OSSE has undertaken observations of gamma-ray lines from several celestial sources. New results have been obtained for solar flare observations, the detection of ^{57}Co from SN 1987a , and the distribution of positron annihilation radiation from the galactic center region. Many of the objectives remain at the limit of the OSSE sensitivity. These include supernovae occurring near distances of 10 Mpc, galactic novae at ~1 kpc, and diffuse line emissions from the interstellar medium. The opportunity for an extended mission with the increased likelihood for nearby novae and supernovae, and extended observations of the galactic plane, should enable many more of these objectives to be achieved.

REFERENCES

Albernhe, F., Leborgne, J. F., Vedrenne, G., Boclet, D., Durouchoux, P., & da Costa, J. M. 1981, Astronomy and Astrophysics, **94**, 214

Anders, E., and Grevesse, N. 1989, Geochim. Cosmochim. Acta, **53**, 197.

Brown, B. L., & Leventhal, M. 1987, Astrophysical Journal, **319**, 637

Bouchet, L., et al. 1991, Astrophysical Journal Letters, **383**, L45

Chapuis, C. G. L., et al. 1991, in "Gamma-Ray Line Astrophysics", ed. P. Durouchoux and N. Prantzos (New York: AIP), 52

Churazov, E., et al. 1993, Astrophys. J., **407**, 752

Clayton, D.D., 1973, Nature Phys. Sci., **244**, 137.

Clayton, D.D., Colgate, S.A., & Fishman, G. 1969, Astrophys. J., **155**, 75

Clayton, D. D., Leising, M. D., The, L. -S., Johnson, W. N. & Kurfess, J. D. 1992, Ap. J. (Lett.) **399**, L141.

Cordier, B., et al. 1993, Astronomy and Astrophysics, **275**, L1

Crannell, C. J., Crannell, H., Ramaty, R. 1979, Ap. J., **229**, 762.

Diehl, R., et al., 1994, in Proc. of Second Compton Symposium, in press.

Gardner, B. M., et al. 1982, in "The Galactic Center", ed. G. R. Riegler and R. D. Blanford (New York: AIP), 144

Gehrels, N., Barthelmy, S. D., Teegarden, B. J., Tueller, J., Leventhal, M., & MacCallum, C. J. 1991, Astrophysical Journal Letters, **375**, L13

Guessoum, N., Ramaty, R., and Lingenfelter, R.E., 1991, ApJ, **378**, 170.

Heindl, W. A., et al. 1993, Astrophysical Journal, **408**, 507

Johnson, W. N., et al. 1993, Astrophysical Journal Supplement, **86**, No. 2, 693

Jung, G.V., et al. 1994, in Proc. of Second Compton Symposium, in press.
Kanbach, G., et al. 1993, Astron. and Ap. Suppl., **97**, 349.
Kozlovsky, B., Murphy, R. J., and Ramaty, R. 1994, in preparation.
Kurfess, J. D. et al. 1992, Ap. J. (Lett.) **399**, L137.
Lei, F., et al. 1993, Astronomy and Astrophysics Supplement, **97**, 189
Leising, M. D. et al. 1994a, Ap. J. (submitted).
Leising, M. D. et al. 1994b, Ap. J. Letters, in press.
Leising, M.D., et al., 1994c, in Proc. of Second Compton Symposium, in press.
Leventhal, M., et al., 1986, Astrophys J. , **302**, 459.
Leventhal, M., Barthelmy, S. D., Gehrels, N., Teegarden, B. J., Tueller, J., & Bartlett, L. M. 1993, Ap. J. Letters, **405**, L25.
Lichti, G. G. et al. 1994, Astron. Ap., in press.
Lingenfelter, R. E., & Ramaty, R, 1982, in The Galactic Center, ed. G.R.Riegler and R.D. Blanford (New York: AIP) 148.
Lingenfelter, R.E. & Hueter, G.J. 1984 in High Energy Transients in Astrophysics, ed. S.E. Woosley (New York: AIP), 558.
Lingenfelter, R. E., & Ramaty, R. 1989, Astrophysical Journal, **343**, 686
Mandzhavidze, N., and Ramaty, R. 1992, Ap. J. (Letters), **396**, L111.
Matz, S.M., Share, G.H., Leising, M.D., Chupp, E.L., Vestrand, W.T., Purcell, W.R., Strickman, M.S., & Reppin, C. 1988, Nature, **331**, 416
Murphy, R. J., et al. 1991, Ap. J., **371**, 793.
Neil, M., et al. 1990, Astrophysical Journal Letters, **356**, L21
Ozernoy, L. M. 1989, in "The Center of the Galaxy" ed. M. Morris (Dordrecht: Kluwer Academic), 555
Paciesas, W. S., Cline, T. L., Teegarden, B. J., Tueller, J., Durouchoux, P., & Hameury, J. M. 1982, Astrophysical Journal Letters, **260**, L7
Purcell, W. R., Grabelsky, D. A., Ulmer, M. P., Johnson, W. N., Kinzer, R. L., Kurfess, J. D., Strickman, M. S., & Jung, G. V. 1993a, in "Proc. Compton Symposium", ed. M. Friedlander & N. Gehrels (New York: AIP), 107.
Purcell, W. R., Grabelsky, D. A., Ulmer, M. P., Johnson, W. N., Kinzer, R. L., Kurfess, J. D., Strickman, M. S., & Jung, G. V. 1993b, Astrophysical Journal Letters, **413**, L85
Purcell, W.R., et al. 1994, in Proc. of Second Compton Symposium, in press.
Ramaty, R., & Lingenfelter, R. E. 1979, Nature, **278**, 127
Ramaty, R., et al. 1993, Adv. Space. Res. (COSPAR), 13, No. 9, p. 275.
Ramaty, R., Leventhal, M., Chan, K. W., & Lingenfelter, R. E. 1992, Astrophysical Journal Letters, **392**, L63
Ramaty, R., Skibo, J.G. & Lingenfelter, R.E. 1994, Ap. J. Suppl., in press.
Rees, M. J. 1982, in "The Galactic Center", ed. G. R. Riegler and R. D. Blanford (New York: AIP), 166
Share, G. H., Leising, M. D., Messina, D. C., & Purcell, W. R. 1990, Astrophysical Journal Letters, **358**, L45
Signore, M., & Vedrenne, G. 1988, Astronomy and Astrophysics, **201**, 379
Sturrock, P. A. 1971, Astrophysical Journal, **164**, 529
Sunyaev, R., et al. 1991, Astrophysical Journal Letters, **383**, L49
Teegarden, B.J., 1994, Ap J. Suppl., in press.
Tueller, J. 1993, in "Proc. Compton Symposium", ed. M. Friedlander & N. Gehrels (New York: AIP), 97.
Woosley, S. E., & Pinto, P. E. 1988, in "Nuclear Spectroscopy of Astrophysical Sources", ed. N. Gehrels and G. H. Share (New York: AIP), 98